JOURNAL OF NATURAL PRODUCTS

Article

Cite This: J. Nat. Prod. XXXX, XXX, XXX−XXX

pubs.acs.org/jnp

Secondary Metabolites from the Fungus *Dictyosporium* sp. and Their MALT1 Inhibitory Activities

Trong D. Tran,[†,¶] Brice A. P. Wilson,[†] Curtis J. Henrich,[†,‡] Louis M. Staudt,[§] Lauren R. H. Krumpe,[†,‡] Emily A. Smith,[†,‡] Jarrod King,[⊥] Karen L. Wendt,[⊥] Alberto M. Stchigel,[∥] Andrew N. Miller,[#] Robert H. Cichewicz,[⊥] Barry R. O'Keefe,[†,□] and Kirk R. Gustafson*[,†]

[†]Molecular Targets Program, Center of Cancer Research, National Cancer Institute, Frederick, Maryland 21701-1201, United States

[‡]Basic Science Program, Leidos Biomedical Research, Inc., Frederick National Laboratory for Cancer Research sponsored by the National Cancer Institute, Frederick, Maryland 21702-1201, United States

[§]Lymphoid Malignancies Branch, Center for Cancer Research, National Cancer Institute, Bethesda, Maryland 20892, United States

[⊥]Natural Products Discovery Group, Department of Chemistry and Biochemistry, University of Oklahoma, Norman, Oklahoma 73019-5251, United States

[∥]Mycology Unit, Universitat Rovira i Virgili, C/Sant Llorenç 21, 43201 Reus, Spain

[#]Illinois Natural History Survey, University of Illinois, 1816 South Oak Street, Champaign, Illinois 61820-6970, United States

[□]Natural Products Branch, Developmental Therapeutics Program, Division of Cancer Treatment and Diagnosis, National Cancer Institute, Frederick, Maryland 21701-1201, United States

Supporting Information

ABSTRACT: Bioassay-guided separation of an extract from a *Dictyosporium* sp. isolate led to the identification of six new compounds, **1**−**6**, together with five known compounds, **7**−**11**. The structures of the new compounds were primarily established by extensive 1D and 2D NMR experiments. The absolute configurations of compounds **3**−**6** were determined by comparison of their experimental electronic circular dichroism (ECD) spectra with DFT quantum mechanical calculated ECD spectra. Compounds **3**−**5** possess novel structural scaffolds, and biochemical studies revealed that oxepinochromenones **1** and **7** inhibited the activity of MALT1 protease.

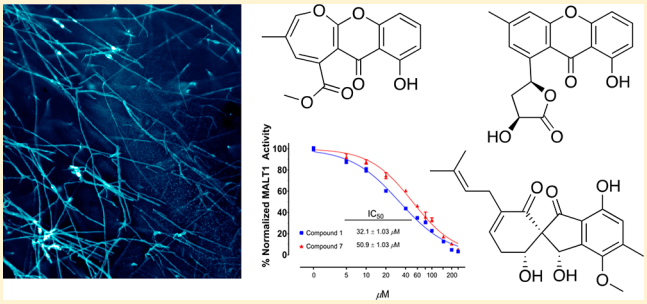

Lymphoma describes a group of hematologic malignancies that develop primarily from T cells or B cells, and it is one of the most frequent types of cancer in the United States.[1,2] Lymphomas comprise two subtypes, Hodgkin and non-Hodgkin lymphoma, of which non-Hodgkin lymphoma accounts for around 90% of all cases.[3] Approximately 85% of all non-Hodgkin lymphomas are of B cell origin,[3] and of these lymphomas, activated B-cell-like diffuse large B cell lymphoma (ABC-DLBCL) is one of the most aggressive. ABC-DLBCL tends to be more resistant to chemotherapeutic treatments and has been reported to be biologically dependent on the proteolytic activity of the mucosa-associated lymphoid tissue lymphoma translocation 1 (MALT1) protease.[4] MALT1 is a paracaspase family protease with unusual arginine-specific catalytic activity that cleaves multiple substrates to promote lymphocyte proliferation and survival via an NFκB signaling pathway.[5] MALT1 is recognized as a promising potential drug target to develop new chemotherapeutic treatments for certain lymphomas.[6] It was found that inhibition of MALT1 protease activity by substrate-mimic tetrapeptide z-VRPR-fmk, which covalently modifies MALT1, caused selective toxicity for ABC-DLBCL cell lines.[7] Synthetic small-molecule inhibitors of MALT1 including a novel triazol (MI-2)[8] and phenothiazines (mepazine, thioridazine, and promazine)[9] displayed selective inhibition against ABC-DLBCL cell lines and were also effective in xenograft models.[8,9] More recently, other new classes of MALT1 inhibitors have been discovered such as β-lapachone and pyrazolo pyrimidine derivatives.[10,11]

As a part of our effort to discover new MALT1 inhibitory natural products, an extract from the fungus *Dictyosporium* sp. was screened and found to inhibit MALT1 proteolytic activity. Members of this fungal genus have been isolated worldwide from sources such as dead wood, decaying leaves, and palm materials,[12] and 46 species have been characterized so far.[13] In spite of its wide occurrence, no chemical investigations of this fungal genus have been previously reported.[14] This paper describes the isolation and structural elucidation of six new

Received: October 19, 2018

DOI: 10.1021/acs.jnatprod.8b00871
J. Nat. Prod. XXXX, XXX, XXX−XXX

compounds and five known metabolites from a soil-derived *Dictyosporium* isolate. Three novel molecular scaffolds were found in this study, and the MALT1 inhibitory activities of the isolated compounds were also evaluated.

RESULTS AND DISCUSSION

The *Dictyosporium* sp. extract was initially chromatographed on a Diol MPLC column and then further purified by C_{18} reversed-phase HPLC to yield six new (**1**–**6**) and five known compounds (**7**–**11**).

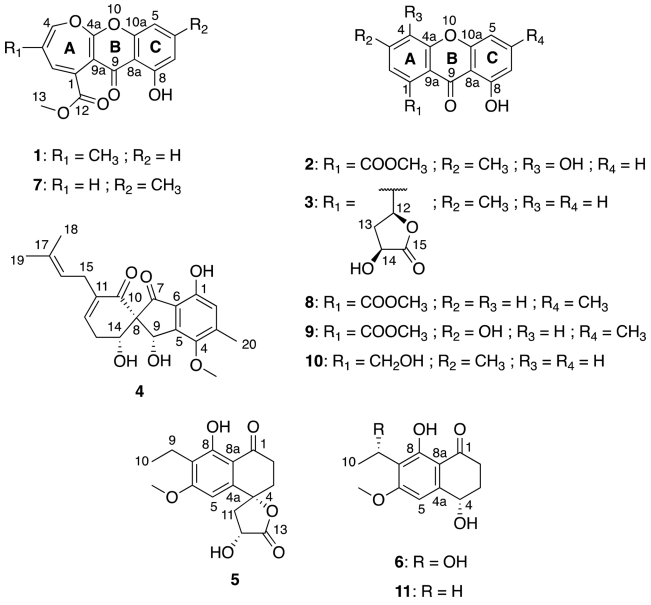

Compound **1** was obtained as an optically inactive white powder. The (+)-HRESIMS spectrum displayed a protonated molecular ion $[M + H]^+$ at m/z 301.0708, corresponding to a molecular formula of $C_{16}H_{12}O_6$ with 11 double-bond equivalents. The IR spectrum showed strong absorptions for hydroxy (3442 cm^{-1}) and ester carbonyl groups (1716 and 1653 cm^{-1}). The ^1H NMR spectrum (Table 1) showed signals for an exchangeable proton (δ_H 12.22), five aromatic or olefinic protons (δ_H 7.52, 6.93, 6.86, 6.83, and 6.22), a methoxy (δ_H 3.82), and a methyl (δ_H 1.81) group. The combined ^{13}C NMR and HSQC data (Table 1) indicated the presence of 16 carbons including two carbonyls (δ_C 182.8 and 167.0), seven nonprotonated sp^2 carbons (δ_C 162.9, 161.1, 153.8, 129.3, 125.8, 109.6, and 104.8), five sp^2 methines (δ_C 141.8, 135.9, 135.5, 112.7, and 107.0), a methoxy carbon (δ_C 52.7), and an aliphatic methyl carbon (δ_C 15.8). A 1,2,3-trisubstituted benzene was deduced based on COSY correlations from H-6 to H-5 and H-7 and HMBC correlations of H-5/C-8a, H-7/C-8a, and H-6/C-8, C-10a. A hydroxy group (8-OH) and a ketone (C-9) were attached at C-8 and C-8a, respectively, due to HMBC correlations of 8-OH/C-8, C-8a, C-9; H-5/C-9; and H-7/C-9. Although all of the HMBC correlations to C-9 were through four bonds, acquisition of the HMBC data set with the experiment optimized for small heteronuclear couplings ($^nJ_{XH}$ = 2.0 Hz) facilitated detection of these key correlations. The deshielded resonance of 8-OH (δ_H 12.22) was indicative of an intramolecular hydrogen bond with the C-9 ketone, which provided further support for this assignment. HMBC correlations of H-2/C-1, C-4, C-9a, C-12; H-4/C-4a; H_3-11/C-2, C-3, C-4; and H_3-13/C-12 helped establish an oxepin ring that was substituted with a methyl carboxylate at C-1 and a methyl group at C-3 (Figure 1). The remaining oxygen atom was placed between C-4a (δ_C 162.9) and C-10a (δ_C 153.8), whose chemical shifts were characteristic of oxygen-substituted sp^2 carbons. The two remaining nonprotonated carbons, C-9 and C-9a, were connected to

Table 1. NMR Spectroscopic Data (^1H 600 MHz, ^{13}C 150 MHz) for Compounds 1–3

	1[a]		2[a]		3[b]	
pos.	δ_C, type	δ_H (J in Hz)	δ_C, type	δ_H (J in Hz)	δ_C, type	δ_H (J in Hz)
1	129.3, C		124.1, C		142.3, C	
2	135.9, CH	6.93, s	125.5, CH	7.15, s	120.8, CH	7.19, s
3	125.8, C		131.0, C		147.4, C	
4	141.8, CH	6.22, s	143.5, C		117.6, CH	7.47, s
4a	162.9, C		143.9, C		157.2, C	
5	107.0, CH	6.86, d (8.4)	106.6, CH	6.96, d (8.4)	106.7, CH	7.05, d (8.4)
6	135.5, CH	7.52, t (8.4)	137.0, CH	7.61, dd (7.8, 8.4)	137.3, CH	7.72, t (8.4)
7	112.7, CH	6.83, d (8.4)	111.7, CH	6.83, d (8.4)	110.3, CH	6.81, d (8.4)
8	161.1, C		162.2, C		161.0, C	
8a	109.6, C		108.8, C		108.9, C	
9	182.8, C		181.0, C		182.8, C	
9a	104.8, C		116.2, C		114.2, C	
10a	153.8, C		155.1, C		155.0, C	
11	15.8, CH_3	1.81, s	16.2, CH_3	2.42, s	21.7, CH_3	2.49, s
12	167.0, C		169.8, C		76.0, CH	6.63, dd (4.2, 8.4)
13	52.7, CH_3	3.82, s	53.2, CH_3	3.99, s	38.5, CH_2	2.37, m
						2.74, dt (8.4, 13.2)
14					65.5, CH	4.35, q (6.6)
15					177.1, C	
4-OH				6.06, s		
8-OH		12.22, s		12.32, s		12.64, br s
14-OH						6.08, d (5.4)

[a]Recorded in $CDCl_3$. [b]Recorded in DMSO-d_6.

DOI: 10.1021/acs.jnatprod.8b00871
J. Nat. Prod. XXXX, XXX, XXX−XXX

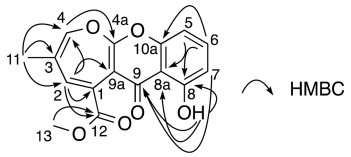

Figure 1. Key HMBC correlations for fusidienol B (**1**).

complete ring B and fulfill the molecular formula requirements. Compound **1** was thus established to be a new positional isomer of fusidienol A (**7**),[15] so it was named fusidienol B. Fusidienol A (**7**) was also isolated from the *Dictyosporium* sp. extract, and it provided NMR data that closely corresponded with the NMR data for **1** (Supporting Information). Fusidienol B (**1**) is only the fourth natural product that shares the 6*H*-oxepino[2,3-*b*]chromen-6-one skeleton that is found in fusidienol A,[15] fusidienol,[16] and microsphaeropsone C.[17]

Compound **2** was isolated as a white powder, and the molecular formula based on (+)-HRESIMS of $C_{16}H_{12}O_6$ was isomeric with **1**. The ^{1}H NMR data of **2** (Table 1) were quite similar to those of **1**, except for the loss of an aromatic proton at δ_H 6.22 in **1** and the appearance of an exchangeable proton at δ_H 6.06 in **2**. Following 1D and 2D NMR analysis, the same 1,2,3-trisubstituted benzene moiety (ring C) seen in **1**, with a hydroxy group at C-8 (δ_H 12.32), a carbonyl C-9 (δ_C 181.0) substituted on C-8a, and oxygenation at C-10a (δ_C 155.1), was confirmed. The chemical shifts of the six remaining aromatic carbons at δ_C 143.9, 143.5, 131.0, 125.5, 124.1, and 116.2 and the more shielded resonance of C-4a (δ_C 143.9) compared to C-4a (δ_C 162.9) in **1** indicated they constituted a benzene ring (ring A), not an oxepin system as seen in **1**.[18] Key HMBC correlations (Figure 2) of H-2/C-9, C-12; H_3-11/C-2, C3, C4;

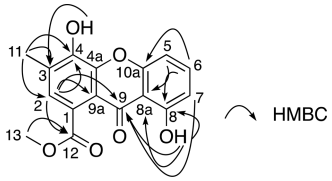

Figure 2. Key HMBC correlations for dictyosporixanthone A (**2**).

4-OH/C-3; and H_3-13/C-12 supported a pentasubstituted benzene ring with a methyl carboxylate (δ_C 169.8), a methyl (δ_C 16.2), a hydroxy group 4-OH (δ_H 6.06), and a carbonyl C-9 (δ_C 181.0), substituted at C-1, C-3, C-4, and C-9a, respectively. An ether connection was inferred between the two oxygenated aromatic carbons C-4a and C-10a to satisfy molecular formula considerations. Compound **2** was thus elucidated as a new xanthone and named dictyosporixanthone A. Dictyosporixanthone A (**2**) could be a precursor of **1** via epoxidation and rearrangement processes.[15] In fungi, the same biogenetic relationship between the xanthone ring system and the ring-extended oxepin has been proposed previously.[15]

Compound **3** was purified as a light yellow powder and gave a protonated molecular ion $[M + H]^+$ in the (+)-HRESIMS spectrum at m/z 327.0855 that established a molecular formula of $C_{18}H_{14}O_6$. NMR analyses confirmed that **3** belonged to the same xanthone structural class. Additional NMR signals corresponding to an exchangeable proton (δ_H 6.08), two oxygenated methines (δ_H/δ_C 6.63/76.0 and 4.35/65.5), a methylene (δ_H/δ_C 2.37 and 2.74/38.5), and a carbonyl carbon (δ_C 177.1) were observed in the ^{1}H and ^{13}C spectra. COSY and HMBC data and the requirement for one additional unsaturation equivalent indicated these resonances constituted a γ-lactone system. Key HMBC correlations from H-12 (δ_H 6.63) to C-1, C-2, and the ester carbonyl C-15 (δ_C 177.1) and H-13/C-1 supported the γ-lactone and confirmed its connection to the xanthone moiety at C-1 (Figure 3A). A key NOESY correlation between H-12 and H-14 placed these protons on the same face of the γ-lactone ring. The experimental electronic circular dichroism (ECD) spectrum of **3** corresponded most closely with the calculated ECD of (12*S*,14*S*)-**3** (Figure 3B), which enabled the assignment of the absolute configuration for **3** as (12*S*,14*S*)-dictyosporixanthone B. With ring A of the xanthone core connected to a γ-lactone substituent, dictyosporixanthone B (**3**) possesses a new heterocyclic skeleton that has not been found in previously reported xanthones.[14]

Compound **4** was purified as a white powder, and its molecular formula was determined to be $C_{21}H_{24}O_6$ from (+)-HRESIMS data. Combined ^{1}H, ^{13}C, and HSQC NMR data (Table 2) indicated the presence of two carbonyls (δ_C 201.1 and 196.5), two oxygenated sp^2 carbons (δ_C 150.9 and 148.3), five additional nonprotonated sp^2 carbons (δ_C 146.1, 140.9, 138.3, 132.3, and 123.1), three sp^2 methines (δ_C 141.7, 121.3, and 118.0), one quaternary carbon (δ_C 71.5), two oxymethines (δ_C 67.8 and 66.2), two methylenes (δ_C 32.3 and 27.3), one methoxy (δ_C 60.5), and three aliphatic methyls (δ_C 25.5, 17.5, and 16.2). COSY analysis revealed three isolated spin systems including H-9−OH, H-12−H_2-13−H-14−OH, and H_2-15−H-16 (Figure 4A). HMBC correlations between H-13/C-11 and H-12/C-10 revealed the presence of an α,β-unsaturated ketone connected to an allylic methylene (C-13).

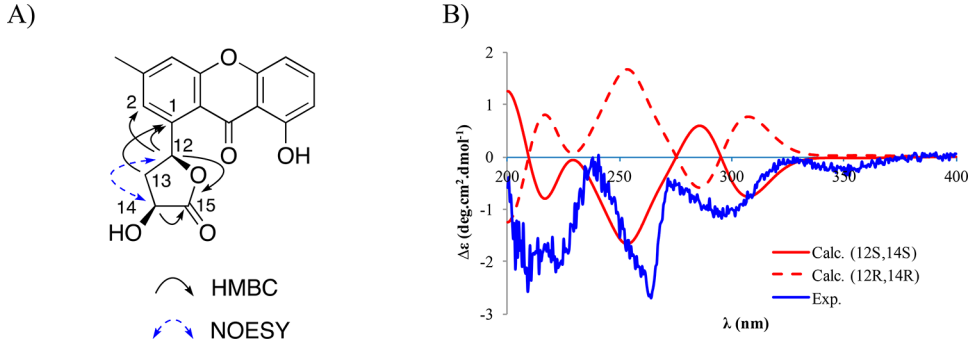

Figure 3. (A) Key HMBC and NOESY correlations of **3**. (B) Experimental ECD spectrum of **3** and calculated ECD spectra of (12*S*,14*S*)-**3** and (12*R*,14*R*)-**3**.

DOI: 10.1021/acs.jnatprod.8b00871
J. Nat. Prod. XXXX, XXX, XXX−XXX

Table 2. NMR Spectroscopic Data (^{1}H 600 MHz, ^{13}C 150 MHz) for 4 Recorded in DMSO-d_6

position	δ_C, type	δ_H (J in Hz)	COSY	ROESY	HMBC
1	150.9, C				
2	118.0, CH	6.66, s		20	4, 6, 20, 1,[c] 7[c]
3	140.9, C				
4	148.3, C				
5	146.1, C				
6	123.1, C				
7	201.1, C				
8	71.5, C				
9	66.2, CH	5.69, d (7.8)	9-OH	13α, 14,[b] 14-OH,[b] 4-OCH$_3$	4, 5, 6, 7, 8, 10, 14, 3[c]
10	196.5, C				
11	138.3, C				
12	141.7, CH	6.62, d (6.0)	13β	14,[b] 15α	10, 14, 15
13	32.3, CH$_2$	H$_\alpha$: 2.68, m	13β, 14	9	
		H$_\beta$: 2.62, dt (6.0, 6.0, 18.0)	12, 13α, 14	14,[b] 14-OH[b]	8, 11, 12, 14
14	67.8, CH	4.34, m	13α, 13β, 14-OH	9,[b] 12,[b] 13β,[b] 16[b,c]	9
15	27.3, CH$_2$	H$_\alpha$: 2.68, m	15β, 16	12, 18	
		H$_\beta$: 2.76, dd (7.2, 15.6)	15α, 16		10, 11, 12, 16, 17
16	121.3, CH	5.07, t (7.2)	15α, 15β	19	15, 18, 19
17	132.3, C				
18	17.5, CH$_3$	1.56, s		15α	16, 17, 19
19	25.5, CH$_3$	1.67, s		16	16, 17, 18
20	16.2, CH$_3$	2.22, s		2, 9	2, 3, 4
4-OCH$_3$	60.5, CH$_3$	3.73, s		9, 20	4
9-OH		5.65, d (7.8)	9		5, 8, 9
1-OH		[a]			
14-OH		5.37, d (4.2)	14	9,[b] 14,[b] 13α,[b] 13β[b]	8

[a]Not observed. [b]1D ROESY. [c]Weak correlation.

A prenyl group was identified by HMBC correlations from H-16 to two allylic methyls (C-18 and C-19) and from H-15, H-18, and H-19 to C-17. HMBC correlations of H-15/C-10 and C-11 established that the prenyl substituent was attached at C-11 of the α,β-unsaturated ketone. The six remaining sp^2 carbons were assigned to form a pentasubstituted benzene ring with a protonated carbon at C-2 having HMBC correlations with C-1, C-4, and C-6. HMBC correlations of H-20/C-2, C-3, and C-4; OCH$_3$/C-4; and H-9/C-4, C-5, and C-6 supported the locations of the C-20 methyl, the methoxy group, and the hydroxy methine carbon C-9 at C-3, C-4, and C-5, respectively. A four-bond HMBC correlation from H-2 to C-7 (δ_C 201.1) established attachment of this ketone carbonyl at C-6. HMBC correlations of H-9/C-8 and C-10; H-13/C-8; 9-OH/C-8; and 14-OH/C-8 facilitated assignment of the spiro junction between an indanone moiety and a cyclohexenone moiety at C-8 (Figure 4A). The relative configuration of **4** was established from 1D and 2D ROESY data. Irradiation of H-14 (δ_H 4.34) resulted in significant enhancements of H-9, H-12, and H-13β, while enhancements of H-9, H-13α, and H-13β were observed when 14-OH (δ_H 5.37) was irradiated. These data together with a key ROESY correlation between H-9 and H-13α (Figure 4B), revealed that two enantiomers, (8*S*, 9*R*, 14*S*) and (8*R*, 9*S*, 14*R*), were possible for **4**. The calculated ECD spectrum of the (8*R*,9*S*,14*R*)-isomer was a good match with the experimental ECD of **4** (Figure 4C), supporting the assignment of the absolute configuration of **4** as (8*R*,9*S*,14*R*)-dictyosporione A. The spiro structure of dictyosporione A (**4**) is related to the spiro architecture of coleophomones A and D.[18−20] However, the significant differences in methyl and prenyl group substitutions and oxygenation between dictyosporione A (**4**) and the coleophomones distinguish this compound as containing a novel structural scaffold.

Compound **5** was purified as a white powder, and its molecular formula was deduced to be $C_{16}H_{18}O_6$ from a sodium adduct ion $[M + Na]^+$ at m/z 329.1004 in the (+)-HRESIMS spectrum. NMR analyses (Table 3) revealed two exchangeable protons (δ_H 13.07 and 6.12), two carbonyl carbons (δ_C 201.9 and 176.3), two nonprotonated sp^2 carbons bearing oxygen (δ_C 163.3 and 160.7), three additional nonprotonated sp^2 carbons (δ_C 145.8, 117.9, and 109.5), one sp^2 methine (δ_C 99.0), one nonprotonated sp^3 carbon bearing oxygen (δ_C 80.5), one oxymethine (δ_C 67.1), four methylenes (δ_C 41.0, 34.2, 31.9, and 15.1), one methoxy (δ_C 56.0), and one methyl group (δ_C 13.1). COSY data defined three isolated spin systems, C-2−C-3, C-9−C-10, and C-11−C-12−OH (Figure 5A). Characteristic chemical shifts of six sp^2 carbons together with HMBC correlations of H-5/C-4a, C-6, C-7, and C-8a; H-9/C-6, C-7, and C-8; H-10/C-7; and the methoxy to C-6 revealed a pentasubstituted benzene ring with hydroxy, ethyl, and methoxy groups assigned at C-8, C-7, and C-6, respectively. HMBC correlations of H-2/C-1, C-8a, and C-4 and H-3/C-1, C-4, and C-4a supported connections from C-2 to C-8a via C-1 and from C-3 to C-4a via C-4, completing the 7-ethyl-8-hydroxy-6-methoxy-3,4-dihydronaphthalen-1(2*H*)-one partial structure, which was similar to that of *O*-methylasparvenone (**11**). An α-hydroxy-substituted γ-lactone was identified as joining the 3,4-dihydronaphthalen-1(2*H*)-one moiety via a spiro ring junction at C-4 based on several considerations including (i) HMBC correlations H-11/C-4, C-4a, C-3, C-13 and H-12/C-13; (ii) molecular formula requirements from mass spectrometry; and (iii) the requirement for one additional degree of unsaturation in the molecule. Thus, the structure of **5** closely correlated with **11**, with an additional spiro fused γ-lactone at C-4 (Figure 5A). Selective NOE experiments for H-11α, H-11β, and H-12 indicated that H-11α was on the same face of the molecule as H-5, while H-11β and H-12 were placed on the same side with H-2β and H-3β (Figure 5B). The calculated ECD spectrum of (4*R*,12*R*)-**5** was in good agreement with the experimentally measured ECD spectrum of **5** (Figure 5C). Therefore, compound **5** was established as (4*R*,12*R*)-dictyosporilactone A. Dictyosporilactone A (**5**) is structurally related to perenniporide A, a spiro naphthelenone isolated from the fungus *Perenniporia* sp.,[21] but compound **5** lacks a $\Delta^{2,3}$ double bond and a methoxy substituent at C-3.

Compound **6** was purified as a white powder, and its molecular formula was established as $C_{13}H_{16}O_5$ by (+)-HRESIMS with an $[M + Na]^+$ ion at m/z 275.0892. This molecular formula had one additional oxygen compared to **11**, and the NMR data of **6** (Table 3) indicated it shared the same 3,4-dihydronaphthalen-1(2*H*)-one moiety with compounds **5** and **11**. The deshielded methine signals at C-9 (δ_H/δ_C 5.16/60.3) together with the doublet proton signal for H$_3$-10 allowed the assignment of an additional hydroxy group at C-9. Comparison of the experimental ECD spectrum of **6** with the calculated ECD of the four stereoisomers (4*S*,9*S*)-**6**, (4*R*,9*R*)-**6**, (4*S*,9*R*)-**6**, and (4*R*,9*S*)-**6** showed the ECD of **6** is compared most

DOI: 10.1021/acs.jnatprod.8b00871
J. Nat. Prod. XXXX, XXX, XXX−XXX

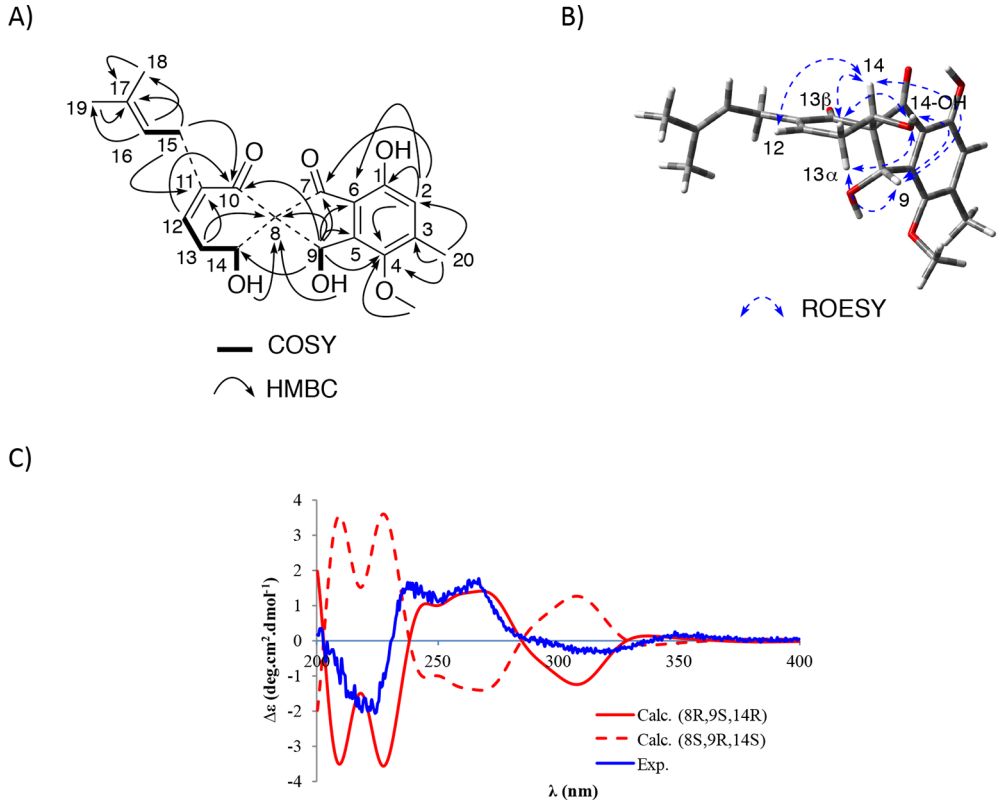

Figure 4. (A) Key HMBC correlations of **4**. (B) Key ROESY correlations of **4**. (C) Experimental ECD spectrum of **4** and calculated ECD spectra of (8*S*,9*R*,14*S*)-**4** and (8*R*,9*S*,14*R*)-**4**.

favorably with the computationally derived data for (4*S*,9*S*)-**6** and (4*S*,9*R*)-**6** with three positive Cotton effects (CEs) at 313, 248, and 214 nm and one negative CE at 282 nm (Figure 6A). However, the CE amplitudes of **6** were notably closer to those of the (4*S*,9*S*)-diastereomer, thus favoring the (4*S*, 9*S*) absolute configuration for **6**. Additional density functional theory (DFT) calculations of the specific rotations (Figure 6B) revealed that (4*S*,9*S*)-**6** had a much closer calculated value compared with the experimentally measured value for **6** ($[\alpha]_D$ = +9). Therefore, compound **6** was proposed as (4*S*,9*S*)-9-hydroxy-*O*-methylasparvenone.

The known compounds fusidienol A (**7**),[15] janthinone (**8**),[22] calyxanthone methyl ester (**9**),[23] 8-hydroxy-1-(hydroxymethyl)-3-methylxanthone (**10**),[24] and *O*-methylasparvenone (**11**)[25] were also isolated from the *D. digitatum* extract, and they were assigned by spectroscopic data comparisons (NMR, MS, and optical rotations) with appropriate literature values. Compounds **1**−**11** were tested for MALT1 inhibitory activity; of these, compounds **1** and **7** exhibited moderate inhibition of MALT1 with IC_{50} values of 32 and 51 μM, respectively (Figure 7). Given their polycyclic conjugated structures, compounds **1** and **7** were also tested for possible fluorescence interference in the assay. Modest fluorescence interference was only observed at concentrations greater than 100 μM (Supporting Information). The other nine compounds **2**−**6** and **8**−**11** showed no significant inhibition at a high-test concentration of 100 μM. This suggested that the 6*H*-oxepino[2,3-*b*]chromen-6-one skeleton plays a key role in the inhibition of MALT1 protease activity. In summary, bioassay-guided fractionation of an extract from a *Dictyosporium* sp. isolate resulted in the identification of 11 metabolites in four structural classes, and the two oxepinochromenones **1** and **7** inhibited the proteolytic activity of MALT1 paracaspase. Although their inhibitory activities were modest, fusidienols A (**7**) and B (**1**) represent the first non-quinone natural products active against MALT1, and they could provide a lead scaffold for the development of clinically relevant MALT1 inhibitors.

EXPERIMENTAL SECTION

General Experimental Procedures. Optical rotations ($[\alpha]_D$) were measured on a PerkinElmer 241 polarimeter. UV spectra were obtained on an Agilent 8453 UV−vis spectrophotometer, ECD spectra were measured on an AVIV 420SF circular dichroism spectrometer, and IR spectra were obtained with a PerkinElmer Spectrum 2000 FT-IR spectrometer. NMR spectra were acquired on a Bruker Avance III spectrometer equipped with a 3 mm cryogenically cooled probe operating at 600 MHz for ^{1}H and 150 MHz for ^{13}C. ^{1}H and ^{13}C NMR spectra were referenced to the residual deuterated solvent peaks at δ_H 7.24 and δ_C 77.2 ($CDCl_3$) and δ_H 2.50 and δ_C 39.5 (DMSO-d_6). HMBC experiments were optimized for $^nJ_{CH}$ = 8.3 or 2.0 Hz. All 2D NMR experiments were acquired with nonuniform sampling (NUS) set to 50%, except for HSQC, which had NUS set to 25%. HRESIMS data were acquired on an Agilent 6520 Accurate Mass Q-TOF instrument. HPLC purifications were performed using a Varian ProStar 218 solvent delivery module HPLC equipped with a Varian ProStar 325 UV−vis detector, operating under Star 6.41 chromatography workstation software. All solvents used for extraction and chromatography were HPLC grade, and the H_2O used was ultrapure water.

Fungal Material. The fungus was obtained from a soil sample collected in Herod, Illinois, USA. The fungal isolate grew slowly on the surfaces of both malt extract and Czapek plates. To aid in the identification of the fungal species, mycelium was collected and subjected to homogenization in TE buffer (10 mM EDTA HCl, 0.1 mM EDTA, pH 8.0) with zirconium oxide beads in a Bullet Blender Storm (MidSci #BBY24M). The isolate was identified as a likely *Dictyosporium* sp. based on analysis of gene sequence data for its

DOI: 10.1021/acs.jnatprod.8b00871
J. Nat. Prod. XXXX, XXX, XXX−XXX

Table 3. NMR Spectroscopic Data (^{1}H 600 MHz, ^{13}C 150 MHz) for Compounds 5 and 6 Recorded in DMSO-d_6

	5		6	
position	δ_C, type	δ_H (J in Hz)	δ_C, type	δ_H (J in Hz)
1	201.9, C		203.4, C	
2	34.2, CH_2	H_α: 2.66, dt (3.6, 18.6)	35.1, CH_2	2.69, m
		H_β: 2.98, m		
3	31.9, CH_2	H_α: 2.26, td (4.2, 13.2)	31.5, CH_2	H_α: 1.91, m
		H_β: 2.32, dt (4.2, 13.2)		H_β: 2.15, m
4	80.5, C		66.3, CH	4.69, dd (3.6, 9.0)
4a	145.8, C		149.6, C	
5	99.0, CH	6.62, s	101.1, CH	6.77, s
6	163.3, C		163.2, C	
7	117.9, C		118.0, C	
8	160.7, C		160.8, C	
8a	109.5, C		109.5, C	
9	15.1, CH_2	2.56, q (7.2)	60.3, CH	5.16, q (6.6)
10	13.1, CH_3	1.01, t (7.2)	22.2, CH_3	1.41, d (6.6)
11	41.0, CH_2	H_α: 2.01, dd (10.2, 13.2)		
		H_β: 3.08, dd (8.4, 13.2)		
12	67.1, CH	4.77, t (9.0, 9.6)		
13	176.3, C			
6-OCH_3	56.0, CH_3	3.91, s	55.9, CH_3	3.88, s
4-OH				5.64, br s
8-OH		13.07, br s		13.18, s
9-OH				[a]
12-OH		6.12, br s		

[a]Not observed.

ribosomal internal transcribed spacer region and the 5.8S rRNA genes (1TS1F-5.8S-ITS4) (GenBank accession number MH882417).[26] BLAST analysis revealed >99% sequence similarity between the soil isolate and several samples in the NCBI database catalogued as *Dictyosporium digitatum*.

Extraction and Isolation. The fungus was grown on Cheerios breakfast cereal supplemented with a 0.3% sucrose solution and 0.005% chloramphenicol in three large mycobags (Unicorn Bags, Plano, TX, USA). The fungus was grown for 6 weeks, whereupon it had achieved complete colonization of the solid substrate. The fungal biomass was extracted by soaking overnight in 8 L of ethyl acetate. The organic extract was subjected to partitioning three times against water (1:1, vol/vol). The ethyl acetate layer was retained and the solvent removed by evaporation *in vacuo*, yielding 5.5 g of vibrant orange-red organic-soluble material. The organic-soluble material was fractionated on a Diol-MPLC column (CombiFlash) with a flow rate of 85 mL/min using a series of organic solvents: (1) 90% hexanes–10% CH_2Cl_2 for 10 min; (2) 95% CH_2Cl_2–5% EtOAc for 10 min; (3) 100% EtOAc for 10 min; (4) 83% EtOAc–17% MeOH for 10 min; and (5) 100% MeOH for 20 min, to give 14 fractions, A–N. Only fractions D and E showed MALT1 inhibitory activity. Fraction D was purified on a C_{18} HPLC column (5 μm, 250 × 21.4 mm) at a flow rate of 9 mL/min with a contiguous elution series that consisted of a linear gradient from 15% CH_3CN–85% H_2O to 50% CH_3CN–50% H_2O over 20 min, isocratic with 50% CH_3CN–50% H_2O for 10 min, and then a linear gradient from 50% CH_3CN–50% H_2O to 100% CH_3CN over 30 min to yield compounds **1** (1 mg, t_R = 25.0 min), **7** (20 mg, t_R = 26.1 min), **10** (1.5 mg, t_R = 27.3 min), and **8** (2 mg, t_R = 29.2 min). Fraction E was chromatographed on a C_{18} HPLC column (5 μm, 250 × 21.4 mm) with the same elution series used for fraction D to obtain **2** (3 mg, t_R = 39.1 min), **3** (0.8 mg, t_R = 43.5 min), **7** (2 mg, t_R = 46.1 min), and **10** (1.8 mg, t_R = 47.3 min). Fraction F was separated on a C_{18} HPLC column (5 μm, 250 × 10 mm) at a flow rate of 4 mL/min with a linear gradient from 20% CH_3CN–80% H_2O to 80% CH_3CN–20% H_2O over 25 min and then from 80% CH_3CN–20% H_2O to 100% CH_3CN in 5 min to afford **4** (1.2 mg, t_R = 16.4 min), **11** (1.6 mg, t_R = 18.5 min), and **9** (2 mg, t_R = 21.5 min). Fractions H and K were also subjected to a C_{18} HPLC column (5 μm, 250 × 10 mm) with a similar program used for fraction F to yield **5** (0.5 mg, t_R = 18.5 min) and **6** (0.3 mg, t_R = 16.2 min), respectively.

*Fusidienol B (**1**):* white powder; UV (MeOH) λ_{max} (log ε) 235 (3.75) and 315 (3.36) nm; IR (NaCl) ν_{max} 3442, 2951, 1716, 1653, 1596, 1489, and 1278 cm^{-1}; ^{1}H and ^{13}C NMR data, Tables 1 and S1 (Supporting Information); (+) HRESIMS m/z 301.0708 $[M + H]^+$ (calcd for $C_{16}H_{13}O_6$, 301.0707, Δ 0.3 ppm).

*Dictyosporixanthone A (**2**):* white powder; UV (MeOH) λ_{max} (log ε) 251 (3.96) and 315 (3.41) nm; IR (NaCl) ν_{max} 3390, 2955, 1718, 1647, 1610, 1507, 1464, 1278, 1226, and 1021 cm^{-1}; ^{1}H and ^{13}C NMR data, Tables 1 and S2 (Supporting Information); (+) HRESIMS m/z 301.0705 $[M + H]^+$ (calcd for $C_{16}H_{13}O_6$, 301.0707, Δ −0.7 ppm).

*Dictyosporixanthone B (**3**):* light yellow powder; $[\alpha]^{22}_D$ −73 (c 0.01, MeOH); UV (MeOH) λ_{max} (log ε) 232 (4.13), 255 (4.04), 287 (3.79) and 358 (3.39) nm; ECD (c 1022 × 10^{-6} M, MeOH) λ_{max} ($\Delta\varepsilon$) 353 (+0.25), 296 (−1.09), 262 (−2.58), 223 (−2.01), and 209 (−2.12) nm; ^{1}H and ^{13}C NMR data, Tables 1 and S3 (Supporting Information); (+) HRESIMS m/z 327.0855 $[M + H]^+$ (calcd for $C_{18}H_{15}O_6$, 327.0863, Δ −2.4 ppm).

*Dictyosporione A (**4**):* white powder; $[\alpha]^{22}_D$ +9 (c 0.05, MeOH); UV (MeOH) λ_{max} (log ε) 216 (4.02), 228 (4.04), 264 (3.76), and 329 (3.33) nm; ECD (c 1120 × 10^{-6} M, MeOH) λ_{max} ($\Delta\varepsilon$) 350 (+0.16), 319 (−0.31), 266 (+1.68), 238 (+1.55), and 223 (−1.98) nm; ^{1}H and ^{13}C NMR data, Table 2; (+) HRESIMS m/z 395.1467 $[M + Na]^+$ (calcd for $C_{21}H_{24}O_6Na$, 395.1465, Δ 0.5 ppm).

*Dictyosporilactone A (**5**):* white powder; $[\alpha]^{22}_D$ +34 (c 0.05, MeOH); UV (MeOH) λ_{max} (log ε) 2.25 (3.94), 288 (3.83), and 335

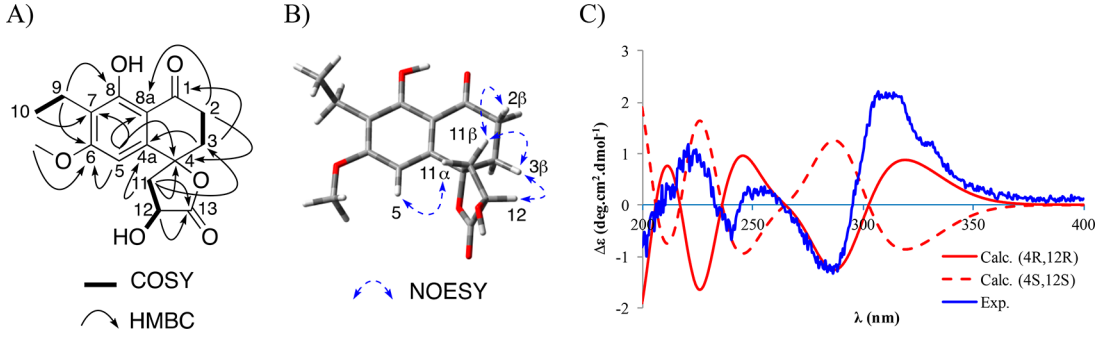

Figure 5. (A) Key HMBC correlations of **5**. (B) Key NOESY correlations of **5**. (C) Experimental ECD spectrum of **5** and calculated ECD spectra of (4*R*,12*R*)-**5** and (4*S*,12*S*)-**5**.

DOI: 10.1021/acs.jnatprod.8b00871
J. Nat. Prod. XXXX, XXX, XXX–XXX

A)

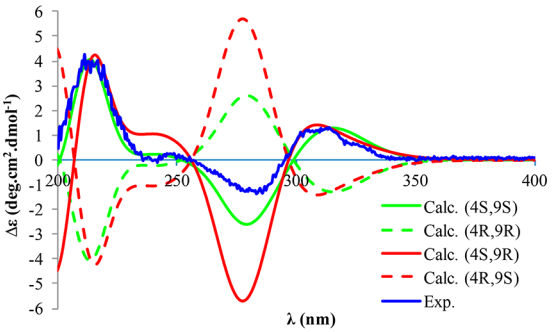

B)

	B3lyp/ aug-cc-pvdz	B3lyp/ aug-cc-pvtz	B3lyp/ 6-31+G(d,p)	B3lyp/ 6-311+G(d,p)
(4*S*, 9*S*)-**6**	**+15**	**+17**	**+18**	**+16**
(4*R*, 9*R*)-**6**	-15	-17	-18	-16
(4*S*, 9*R*)-**6**	+33	+33	+34	+34
(4*R*, 9*S*)-**6**	-33	-33	-34	-34

Figure 6. (A) Experimental ECD spectrum of **6** and calculated ECD spectra of (4*S*,9*S*)-**6**, (4*R*,9*R*)-**6**, (4*S*,9*R*)-**6**, and (4*R*,9*S*)-**6**. (B) Calculated specific rotations using four different basis sets for (4*S*,9*S*)-**6**, (4*R*,9*R*)-**6**, (4*S*,9*R*)-**6**, and (4*R*,9*S*)-**6**.

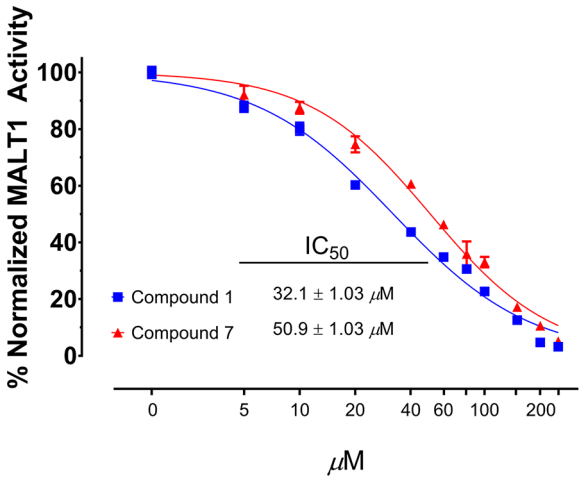

Figure 7. Dose−response curves and IC_{50} values for compounds **1** and **7**. Compounds **1** and **7** were tested in quadruplicate for the ability to inhibit MALT1 protease activity in a fluorescence-based biochemical assay.

(3.30) nm; ECD (c 1089 × 10^{-6} M, MeOH) λ_{max} ($\Delta\varepsilon$) 310 (+2.15), 285 (−1.23), 254 (+0.27), 240 (−0.40), and 221 (+1.00) nm; ^{1}H and ^{13}C NMR data, Tables 3 and S4 (Supporting Information); (+) HRESIMS m/z 329.1004 $[M + Na]^+$ (calcd for $C_{16}H_{18}O_6Na$, 329.0996, Δ 2.4 ppm).

*9-Hydroxy-O-methylasparvenone (**6**):* white powder; $[\alpha]^{22}_D$ +9 (c 0.03, MeOH); UV (MeOH) λ_{max} (log ε) 223 (3.90), 285 (3.78), and 330 (3.27) nm; ECD (c 1323 × 10^{-6} M, MeOH) λ_{max} ($\Delta\varepsilon$) 313 (+1.31), 285 (−1.34), 248 (+0.27), and 214 (+4.00) nm; ^{1}H and ^{13}C NMR data, Tables 3 and S5 (Supporting Information); (+) HRESIMS m/z 275.0892 $[M + Na]^+$ (calcd for $C_{13}H_{16}O_5Na$, 275.0890, Δ 0.7 ppm).

Computational Details. TDDFT ECD calculations for **3**−**6** were performed at 298 K using Maestro and Gaussian 09 software. Molecular mechanics calculations were performed using Macromodel interfaced to the Maestro program (version 2015.3, Schrödinger).[27] All conformational searches used the OPLS_2005 force field. Conformers having internal relative energies within 3 kcal/mol were subjected to geometry optimization on Gaussian 09[28] at the DFT level with the B3LYP functional and the 6-31G(d,p) basis set. Optimized conformers were then subjected to TDDFT calculations in MeOH on Gaussian 09 using the B3LYP functional and the 6-31G(d,p) basis set for **3**, **5**, and **6** and the 6-31+G(d,p) basis set for **4**. All calculations were performed in MeOH solvent. For each conformer, all of the resultant rotational strengths were converted into Gaussian distributions and summed to obtain the final calculated ECD spectrum based on the Boltzmann distribution of each conformer. ECD spectra were generated using the SpecDis program.[29] Optical rotation calculations for the stereoisomers of **6** employed molecular mechanics and quantum chemical calculations for each particular stereoisomer, performed in MeOH with the same procedure as above. Optical rotation calculations were computed at the DFT levels using the B3LYP functional and an array of basis sets including aug-cc-pvdz, aug-cc-pvtz, 6-31+G(d,p), and 6-311+G(d,p). Final calculated optical rotations were obtained from the Boltzmann-weighted average.

MALT1 Assay. Enzymatic expression and activity assays were similar to those described previously.[30] Briefly, DNA encoding human full-length MALT1 isoform A (824 amino acids), NCBI Ref Sequence NM_006785.2, was purchased from GenScript (Piscataway, NJ, USA). An amino terminal nucleotide sequence was added to allow for the TEV protease-mediated cleavage of an affinity tag from the translated construct. The MALT1 ORF plus the TEV recognition site (TEV-MALT1) was then subcloned into the pDONR221 Gateway Expression entry vector (Invitrogen, Grand Island, NY, USA). A glutathione *S*-transferase (GST)-tagged TEV-MALT1 (GST-TEV-MALT1) expression construct was created using the Gateway cloning system by recombining the TEV-MALT1 pDONR221donor vector with pDEST15 using LR Clonase II (Invitrogen). Following IPTG-induced protein expression in *E. coli*, cells were lysed, and GST-TEV-MALT1 was purified according to manufacturer's protocols using a 5 mL GSTrap FF column (GE Healthcare Life Sciences, Piscataway,

DOI: 10.1021/acs.jnatprod.8b00871
J. Nat. Prod. XXXX, XXX, XXX−XXX

NJ, USA). Pooled GST-TEV-MALT1 positive fractions were digested with TEV protease and further purified by size exclusion chromatography using a Sephacryl S200 HR column. MALT1 positive fractions were combined with glycerol (30% final) and frozen at −80 °C until use. The specific activity of MALT1-GST was determined according to published procedures using the covalent MALT1 inhibitor z-VRPR-FMK (Enzo Life Sciences, Farmingdale, NY, USA).[31] For dose−response measurements, MALT1-GST was combined with assay buffer (50 mM Tris HCl pH 7.5, 0.05% CHAPS (w/v), 1 mM DTT, 0.1 mM EGTA 0.8 M sodium citrate) at 1.2× the final concentration (25 nM). A 6× final concentration of 7-amino-4-methylcoumarin-labeled peptide substrate, Ac-LRSR-MCA (Peptides International, Louisville, KY, USA), and increasing concentrations of each compound were prepared in assay buffer. The reaction was initiated by the addition of substrate/compound to the reaction mixture to reach a final reaction concentration of 25 nM MALT1-GST, 150 μM substrate, and 0−250 μM compound. Reaction plates were sealed and placed in a 37 °C incubator for 1 h. Prior to reading, reactions were quenched by the addition of an equal volume of 0.2% sodium dodecyl sulfate (SDS). Quadruplicate quenched reactions were then measured for fluorescence intensity in a Molecular Devices SpectraMax i3X plate reader (Molecular Devices, LLC., San Jose, CA, USA) at 342 nm excitation and 441 nm emission wavelengths. Corning Costar (Corning, NY, USA) black 384-well fluorescence compatible polypropylene plates were used for all fluorescence experiments. The covalent MALT1 inhibitor VRPR-FMK (valine-arginine-proline-arginine-fluoromethyl ketone) was used as a positive control (IC_{50} = 16 nM).

In parallel to the enzymatic assays, each compound was also tested for the ability to directly modulate the fluorescence of 7-amino-4-methylcoumarin (AMC, Sigma-Aldrich, St. Louis, MO, USA), the fluorophore cleaved from the MALT1 substrate in the enzymatic assay. This assay was designed to determine if nonspecific interactions of test compounds with the AMC fluorophore were interfering with the evaluation of MALT1 enzyme activity. For this assay, AMC was used in place of the peptide substrate in preparing the compound dose−response dilutions, and this mixture (6× AMC and 6× compound) was diluted to a final concentration of 30 μM AMC and 0−250 μM compound into the assay buffer containing MALT1-GST. Samples were treated identically to those of the enzymatic assay. Collected data were first background corrected by subtracting the average fluorescence of prequenched control reactions from all experimental wells. The background-corrected readings were then normalized as a percentage of the vehicle control reaction according to the following formula:

$$\text{Nomalized \% MALT1 Activity} = 100 \times \left(\frac{\text{RFU}_{\text{compound}}}{\text{RFU}_{\text{vehicle control}}} \right)$$

The normalized data were then directly plotted as a semilog plot, and an IC_{50} value was determined using GraphPad Prism software (GraphPad Software Inc., La Jolla, CA, USA) by nonlinear regression for each compound (I) according to the following equation:

$$\text{\% Normalized Activity} = \frac{100}{(1 + 10^{((\log IC_{50} - \log[I]) \times \text{Hill slope})})}$$

■ ASSOCIATED CONTENT

Supporting Information

The Supporting Information is available free of charge on the ACS Publications website at DOI: 10.1021/acs.jnatprod.8b00871.

1D and 2D NMR data, spectra of **1**−**6**, and biological testing data for all isolated compounds (PDF)

■ AUTHOR INFORMATION

Corresponding Author

*Tel: +1-301-846-5197. Fax: +1-301-846-6851. E-mail: gustafki@mail.nih.gov.

ORCID

Robert H. Cichewicz: 0000-0003-0744-4117
Barry R. O'Keefe: 0000-0003-0772-4856
Kirk R. Gustafson: 0000-0001-6821-4943

Present Address

¶GeneCology Research Centre, Faculty of Science, Health, Engineering and Education, University of the Sunshine Coast, Maroochydore DC, Queensland 4558, Australia.

Notes

The authors declare no competing financial interest.

■ ACKNOWLEDGMENTS

Grateful acknowledgement goes to A. Wamiru for MALT1 assay support and H. Bokesch for assistance with HRMS studies. This research utilized the computational resources of the NIH HPC Biowulf cluster, and it was supported in part by the Intramural Research Program of the NIH, National Cancer Institute, Center for Cancer Research, and with federal funds from the National Cancer Institute, National Institutes of Health, under contract HHSN261200800001E. The research was also supported in part by a grant from the National Cancer Institute (UO1CA182740). The content of this publication does not necessarily reflect the views or policies of the Department of Health and Human Services, nor does mention of trade names, commercial products, or organizations imply endorsement by the U.S. Government.

■ REFERENCES

(1) Siegel, R. L.; Miller, K. D.; Jemal, A. *Ca-Cancer J. Clin.* **2017**, *67*, 7−30.
(2) Tobinai, K.; Klein, C.; Oya, N.; Fingerle-Rowson, G. *Adv. Ther.* **2017**, *34*, 324−356.
(3) Zappasodi, R.; de Braud, F.; Di Nicola, M. *Front. Immunol.* **2015**, *6*, 448.
(4) Fontan, L.; Melnick, A. *Clin. Cancer Res.* **2013**, *19*, 6662−6668.
(5) Hailfinger, S.; Lenz, G.; Thome, M. *Curr. Opin. Chem. Biol.* **2014**, *23*, 47−55.
(6) Young, R. M.; Staudt, L. M. *Cancer Cell* **2012**, *22*, 706−707.
(7) Ferch, U.; Kloo, B.; Gewies, A.; Pfander, V.; Duwel, M.; Peschel, C.; Krappmann, D.; Ruland, J. *J. Exp. Med.* **2009**, *206*, 2313−2320.
(8) Fontan, L.; Yang, C.; Kabaleeswaran, V.; Volpon, L.; Osborne, M. J.; Beltran, E.; Garcia, M.; Cerchietti, L.; Shaknovich, R.; Yang, S. N.; Fang, F.; Gascoyne, R. D.; Martinez-Climent, J. A.; Glickman, J. F.; Borden, K.; Wu, H.; Melnick, A. *Cancer Cell* **2012**, *22*, 812−824.
(9) Nagel, D.; Spranger, S.; Vincendeau, M.; Grau, M.; Raffegerst, S.; Kloo, B.; Hlahla, D.; Neuenschwander, M.; Peter von Kries, J.; Hadian, K.; Dorken, B.; Lenz, P.; Lenz, G.; Schendel, D. J.; Krappmann, D. *Cancer Cell* **2012**, *22*, 825−837.
(10) Lim, S. M.; Jeong, Y.; Lee, S.; Im, H.; Tae, H. S.; Kim, B. G.; Park, H. D.; Park, J.; Hong, S. *J. Med. Chem.* **2015**, *58*, 8491−8502.
(11) Abdel-Magid, A. F. *ACS Med. Chem. Lett.* **2016**, *7*, 205−206.
(12) Goh, T.-K.; Hyde, K. D.; Ho, W. H.; Yanna. *Fungal Divers.* **1999**, *2*, 65−100.
(13) Prasher, I. B.; Verma, R. K. *Phytotaxa* **2015**, *204*, 193−202.
(14) In *Dictionary of Natural Products 25.2 online*; Taylor & Francis Group, 2017.
(15) Singh, S. B.; Ball, R. G.; Zink, D. L.; Monaghan, R. L.; Polishook, J. D.; Sanchez, M.; Pelaez, F.; Silverman, K. C.; Lingham, R. B. *J. Org. Chem.* **1997**, *62*, 7485−7488 .

DOI: 10.1021/acs.jnatprod.8b00871
J. Nat. Prod. XXXX, XXX, XXX−XXX

(16) Singh, S. B.; Jones, E. T.; Goetz, M. A.; Bills, G. F.; Nallin-Omstead, M.; Jenkins, R. G.; Lingham, R. B.; Silverman, K. C.; Gibbs, J. B. *Tetrahedron Lett.* **1994**, *35*, 4693−4696.
(17) Krohn, K.; Kouam, S. F.; Kuigoua, G. M.; Hussain, H.; Cludius-Brandt, S.; Florke, U.; Kurtan, T.; Pescitelli, G.; Di Bari, L.; Draeger, S.; Schulz, B. *Chem. - Eur. J.* **2009**, *15*, 12121−12132.
(18) Wilson, K. E.; Tsou, N. N.; Guan, Z.; Ruby, C. L.; Pelaez, F.; Gorrochategui, J.; Vicente, F.; Onishi, H. R. *Tetrahedron Lett.* **2000**, *41*, 8705−8709.
(19) Nicolaou, K. C.; Montagnon, T.; Vassilikogiannakis, G. *Chem. Commun.* **2002**, *21*, 2478−2479.
(20) Nicolaou, K. C.; Montagnon, T.; Vassilikogiannakis, G.; Mathison, C. J. *J. Am. Chem. Soc.* **2005**, *127*, 8872−8888.
(21) Feng, Y.; Wang, L.; Niu, S.; Li, L.; Si, Y.; Liu, X.; Che, Y. *J. Nat. Prod.* **2012**, *75*, 1339−1345.
(22) Macias, M.; Gamboa, A.; Ulloa, M.; Toscano, R. A.; Mata, R. *Phytochemistry* **2001**, *58*, 751−758.
(23) Hamasaki, T.; Kimura, Y. *Agric. Biol. Chem.* **1983**, *47*, 163−165.
(24) Hein, S. M.; Gloer, J. B.; Koster, B.; Malloch, D. *J. Nat. Prod.* **1998**, *61*, 1566−1567.
(25) Bos, M.; Canesso, R.; Inoue-Ohga, N.; Nakano, A.; Takehana, Y.; Sleight, A. J. *Bioorg. Med. Chem.* **1997**, *5*, 2165−2171.
(26) Raja, H. A.; Miller, A. N.; Pearce, C. J.; Oberlies, N. H. *J. Nat. Prod.* **2017**, *80*, 756−770.
(27) *Schrödinger Release 2015-3: MacroModel*, Version 10.9; Schrödinger, LLC: New York, 2015.
(28) Frisch, M. J.; Trucks, G. W.; Schlegel, H. B.; Scuseria, G. E.; Robb, M. A.; Cheeseman, J. R.; Scalmani, G.; Barone, V.; Mennucci, B.; Petersson, G. A.; Nakatsuji, H.; Caricato, M.; Li, X.; Hratchian, H. P.; Izmaylov, A. F.; Bloino, J.; Zheng, G.; Sonnenberg, J. L.; Hada, M.; Ehara, M.; Toyota, K.; Fukuda, R.; Hasegawa, J.; Ishida, M.; Nakajima, T.; Honda, Y.; Kitao, O.; Nakai, H.; Vreven, T.; Montgomery, J. A.; Peralta, J. E.; Ogliaro, F.; Bearpark, M.; Heyd, J. J.; Brothers, E.; Kudin, K. N.; Staroverov, V. N.; Kobayashi, R.; Normand, J.; Raghavachari, K.; Rendell, A.; Burant, J. C.; Iyengar, S. S.; Tomasi, J.; Cossi, M.; Rega, N.; Millam, J. M.; Klene, M.; Knox, J. E.; Cross, J. B.; Bakken, V.; Adamo, C.; Jaramillo, J.; Gomperts, R.; Stratmann, R. E.; Yazyev, O.; Austin, A. J.; Cammi, R.; Pomelli, C.; Ochterski, J. W.; Martin, R. L.; Morokuma, K.; Zakrzewski, V. G.; Voth, G. A.; Salvador, P.; Dannenberg, J. J.; Dapprich, S.; Daniels, A. D.; Farkas, Ö.; Foresman, J. B.; Ortiz, J. V.; Cioslowski, J.; Fox, D. J. *Gaussian 09*; Gaussian, Inc.: Wallingford, CT, 2013.
(29) Bruhn, T.; Schaumlöffel, A.; Hemberger, Y. *SpecDis*, Version 1.63; University of Wuerzburg, Germany, 2015.
(30) Wiesmann, C.; Leder, L.; Blank, J.; Bernardi, A.; Melkko, S.; Decock, A.; D'Arcy, A.; Villard, F.; Erbel, P.; Hughes, N.; Freuler, F.; Nikolay, R.; Alvers, J.; Bomancin, F.; Renatus, M. *J. Mol. Biol.* **2012**, *419*, 4−21.
(31) Hachmann, J.; Salvesen, G. S. *Biochimie* **2016**, *122*, 324−338.

DOI: 10.1021/acs.jnatprod.8b00871
J. Nat. Prod. XXXX, XXX, XXX−XXX